Influence of Contact Stress Model on the Stability of Bridge Abutment

Radim Cajka, David Pustka and David Sekanina

Additional information is available at the end of the chapter

http://dx.doi.org/10.5772/66803

Abstract

This chapter deals with the behaviour of an abutment pier on subsoil subjected to flood changes. The floods increase the cross-section of the river bed and change the properties of the foundation soil under the foundation. First, the soil saturates with water. Then, fine-grained particles will wash away and finally parts of the basement rock will be washed off. Finite element method has been used for the calculation of the interaction between the foundation and the subsoil. The foundation has been modelled in a 2D environment using spatial components. For the subsoil, an element with effects of an elastic foundation has been used. The stiffness of the bedrock has been characterized by the C parameter. The chapter describes situations related to the collapse of the structure.

Keywords: bridge, abutment pier, basement rock, floods, soil-structure, interaction

1. Introduction

Unflagging growth of anthropogenic activities has been causing changes in the Earth's climate. These changes have led to the changes of weather in comparison to the past. Changes in weather frequently have brought increased values of loads (e.g. due to wind, snow and water) which can significantly influence reliability (see, e.g. Tikalsky et al., 2005; Pustka et al., Raizer, 2009; Briaud et al., 2014; Králik and Králik, 2014; Markova et al., 2014; Pustka, 2014; Janas et al., 2015; Pustka, 2015; Koteš et al., 2016) of (civil) engineering structures. To assure required level of reliability of these structures, it is necessary to deal with this issue. Climate's changes have brought, among others, heavier precipitations which have led to excessive water flows or even to floods. This unexpected flows of water can significantly damage bridge structures crossing these watercourses (see, e.g. Cajka and Manasek, 2005; Link et al., 2008; Pasiok and

Stilger-Szydlo, 2010; Burns et al., 2011; Wang et al., 2011; Yu et al., 2011; Khosronejad et al., 2012; Collins et al., 2013; Lin et al., 2014; Afzali, 2015; Ehteram and Meymand, 2015; Klinga and Alipour, 2015; Fael et al., 2016; Mohamed et al., 2016). In association with this growing risk, a study examining effects of scour to a bridge abutment was elaborated.

In the following model, an example of a bridge pier (Strasky et al., 2001; Navratil, 2004; CNI, 2005; Parke and Nigel, 2008; Navratil and Zich, 2013; Sucharda and Brozovsky, 2013) is considered. To analyse interaction between the basement rock and foundation (see, e.g. CNI, 1988; CNI, 2004; Cajka et al., 2011; Cajka, 2013a,b,c; Cajka et al., 2014; Unlu et al., 2013; Hrubesova et al., 2015; Lahuta et al., 2015; Hrubesova et al., 2016; Cajka et al., 2016a,b; Labudkova and Cajka, 2016) a parametric study has been created. In the study, the finite element method on elastic subsoil has been utilised. The floods increase the cross-section of the river bed and change the properties of the foundation soil under the foundation (see, e.g. Ettema et al., 2000). In the first stage, the soil saturates with water. In the second stage fine-grained particles will wash away. In the third stage, parts of the basement rock will be washed off.

2. Model example of an abutment pier

2.1. Assumptions of calculation

For the calculation of interaction between the foundation and basement finite element method has been used (FEM consulting, 2002). The foundation has been modelled in a 2D environment using spatial components. For the basement rock, an element with effects of an elastic foundation has been used. The *C* parameter represents properties of the basement rock.

2.2. Subsoil model

The most efficient way for solutions of interaction tasks is a 2D model of the basement rock. Such model represents correctly, through a surface model, deformation properties of the whole mass of the foundation soil. The physical properties are expressed by means of subsoil parameters. The set of the interaction parameters is marked briefly as *C*. The parameters are allocated directly to structure components that are in the contact with the basement rock. The parameters describe the properties that influence the stiffness matrix. To simplify the situation, the *C* parameter can be imagined as the supporting by means of a dense liquid $\gamma = C_{1z}$ (MN m^{-3}) or by means of a set of vertical springs with an infinite density. From the physical point of view, there is not any difference. In case of extreme simplification, the *C* parameter can be imagined as Winkler's elastic foundation model.

2.3. Modelling and description of the structure

As a material for the foundation concrete C16/20 has been considered. Dimensions of the abutment pier are evident from **Figure 1**. The pier has been loaded by the horizontal load-carrying structure of the bridge (forces R_{gk} and R_{qk}). The load developed by the soil and random load of the road that influences the back face of the pier structure, have been introduced by H_k force (see **Figure 1**).

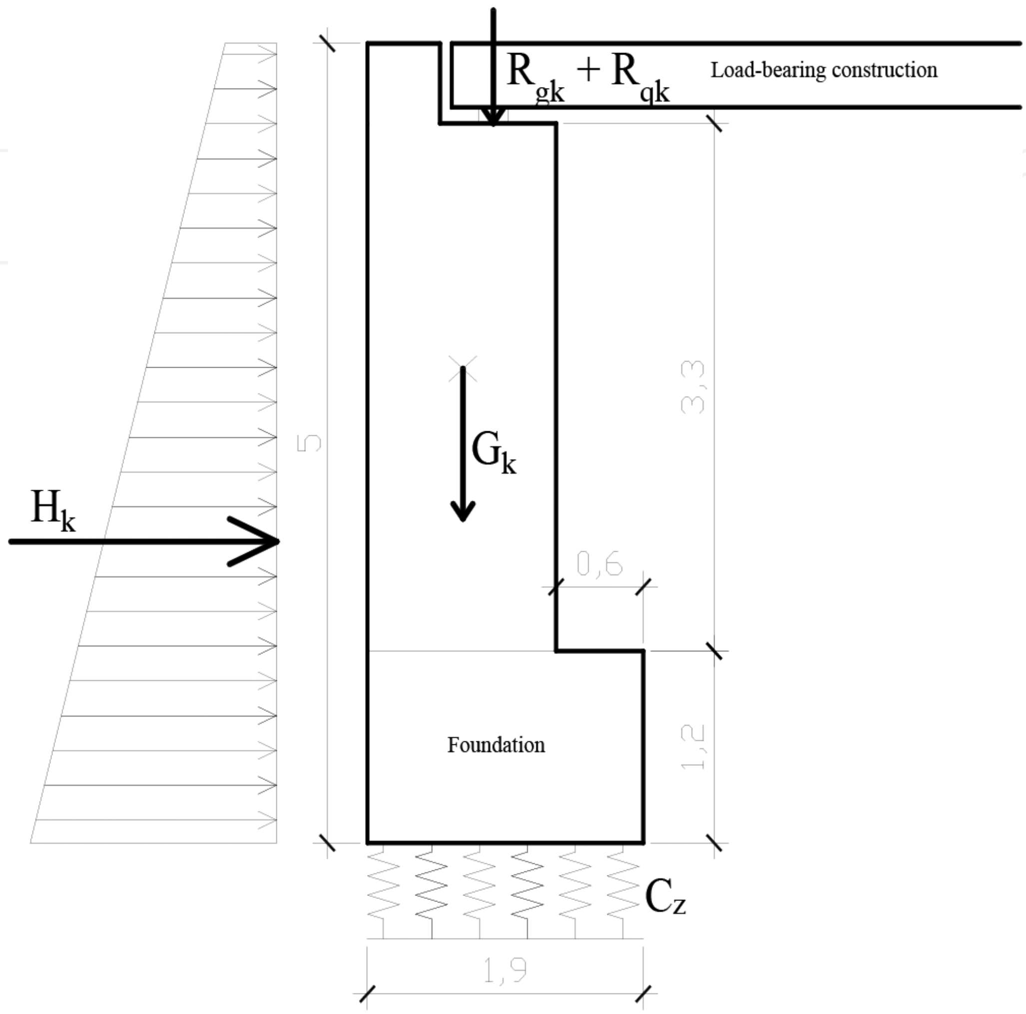

Figure 1. Scheme of the abutment pier with considered loads.

As far as the structure of the abutment pier is concerned, the foundation structure has been used only for the calculation. The loading of the whole upper construction has been re-calculated and simplified. Only the vertical loading and bending moment in the centre of gravity of the stem have been taken into consideration. The basement rock has been modelled using the C_z parameter. For purposes of the calculation, the following reference value has been used: C_z = 25 MN m^{-3}. This rough value is given by characteristic of gravel with fine-grain particles and by the loading and deformation for a specific type of the basement rock. The interaction has been solved for several cases: the value of C_z has changed because of the lower stiffness of the basement rock that was caused by the washing off of the fine-grain particles. In another case, the washing off of the basement rock has been taken into consideration. Finally, the combination of the both cases above has been investigated. **Figure 2** shows the foundation with considered distributions of the basement rock stiffness C_z.

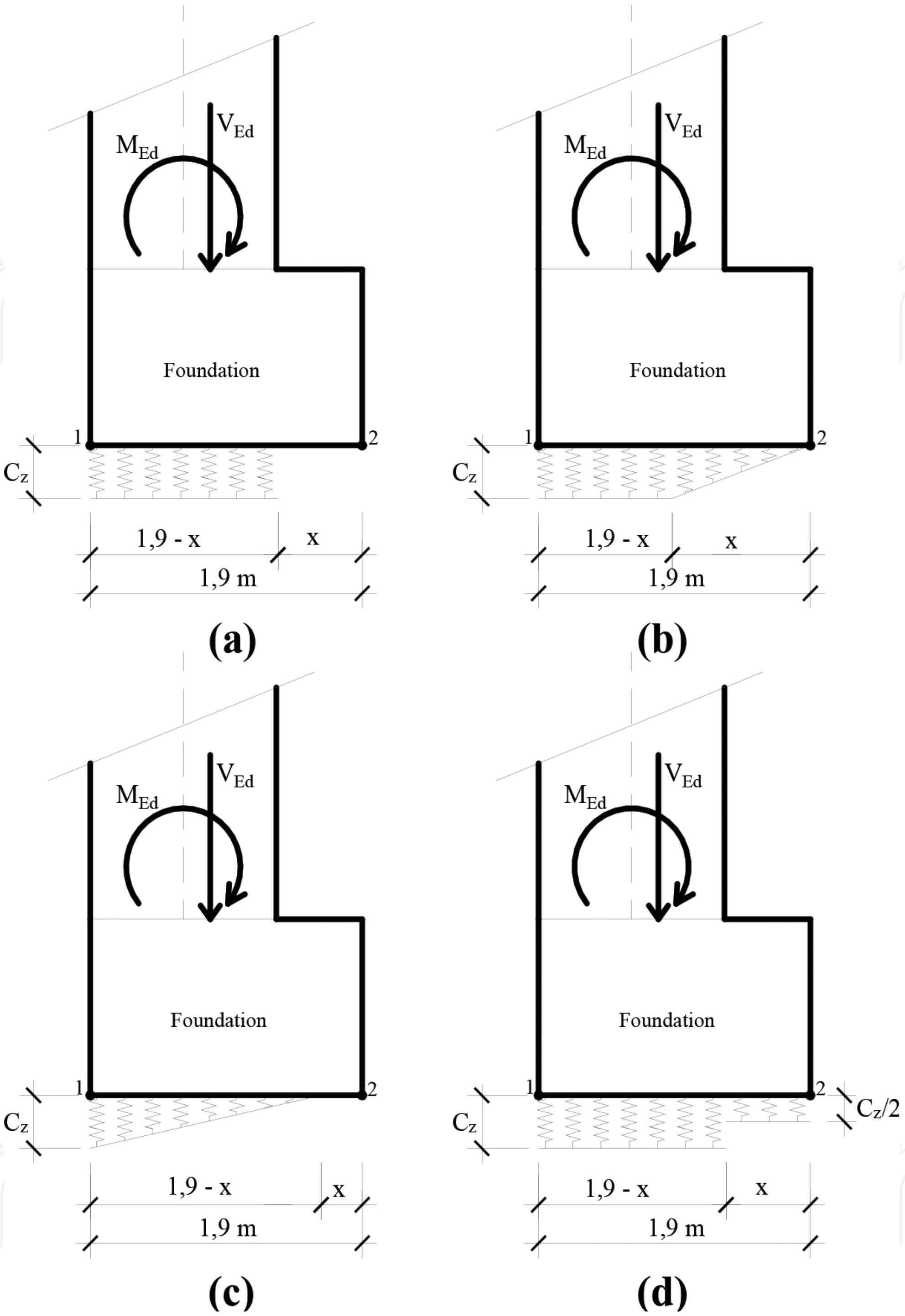

Figure 2. The foundation with considered distributions of the basement rock stiffness C_z.

2.3.1. Partial loss of contact between the foundation and basement rock

The flow of water washes away the basement rock. This reduces the contact surface resulting in increase of the stress in the foundation joint. Because of the non-homogeneous distribution of the tension in the foundation joint, the settlements in points 1 and 2 (see **Figure 2**) are different. Consequently, the foundation joint rotates. **Table 1** shows the settlements of the pier in the points 1 and 2 and the total rotation. Assumed deformation of the foundation is shown in **Figure 3**. Rotation is calculated according to Eq. (1):

$$\varphi = arctg \frac{\Delta w}{b} \quad (1)$$

x [m]	Origin (1.9 – x) [m]	w_1 [mm]	w_2 [mm]	$\Delta w = w_2 - w_1$ [mm]	Rotation of foundation [deg]	Max. stress on foundation surface [MPa]
0.0	1.9	6.92	11.98	5.06	0.152	0.299
0.1	1.8	5.50	14.95	9.46	0.285	0.361
0.2	1.7	3.68	19.07	15.39	0.464	0.435
0.3	1.6	1.35	24.81	23.46	0.707	0.526
0.4	1.5	–1.66	32.88	34.54	1.042	0.638
0.5	1.4	–5.57	44.37	49.94	1.506	0.778
0.6	1.3	–10.71	60.99	71.70	2.163	0.955
0.7	1.2	–17.56	85.45	103.01	3.109	1.182
0.8	1.1	–26.83	122.29	149.12	4.506	1.479
0.9	1.0	–39.65	179.31	218.96	6.632	1.877
1.0	0.9	–57.82	270.62	328.44	10.004	2.426

Table 1. Deformation of the foundation for the case 'a'.

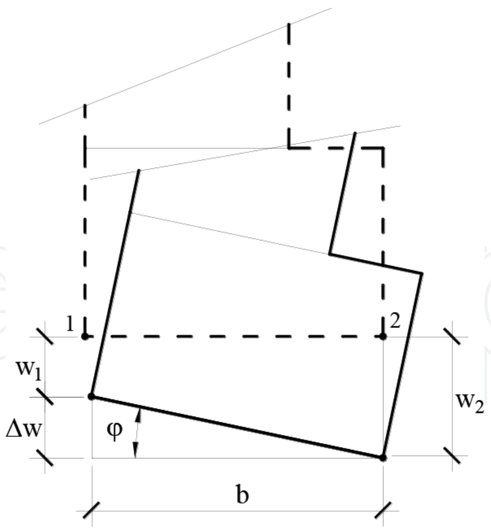

Figure 3. Assumed deformation of the foundation.

Figure 2 shows the x-coordinates related to considered distribution of the basement rock stiffness C_z. When the contact surface is reduced to a certain level, tensile forces are generated. Elements, where tensile stress appeared, have been excluded from the calculation. **Figure 4**

shows the chart for the calculation where the tension in the contact surface is taken into account (case (a*)). For case (a), an iteration method has been used.

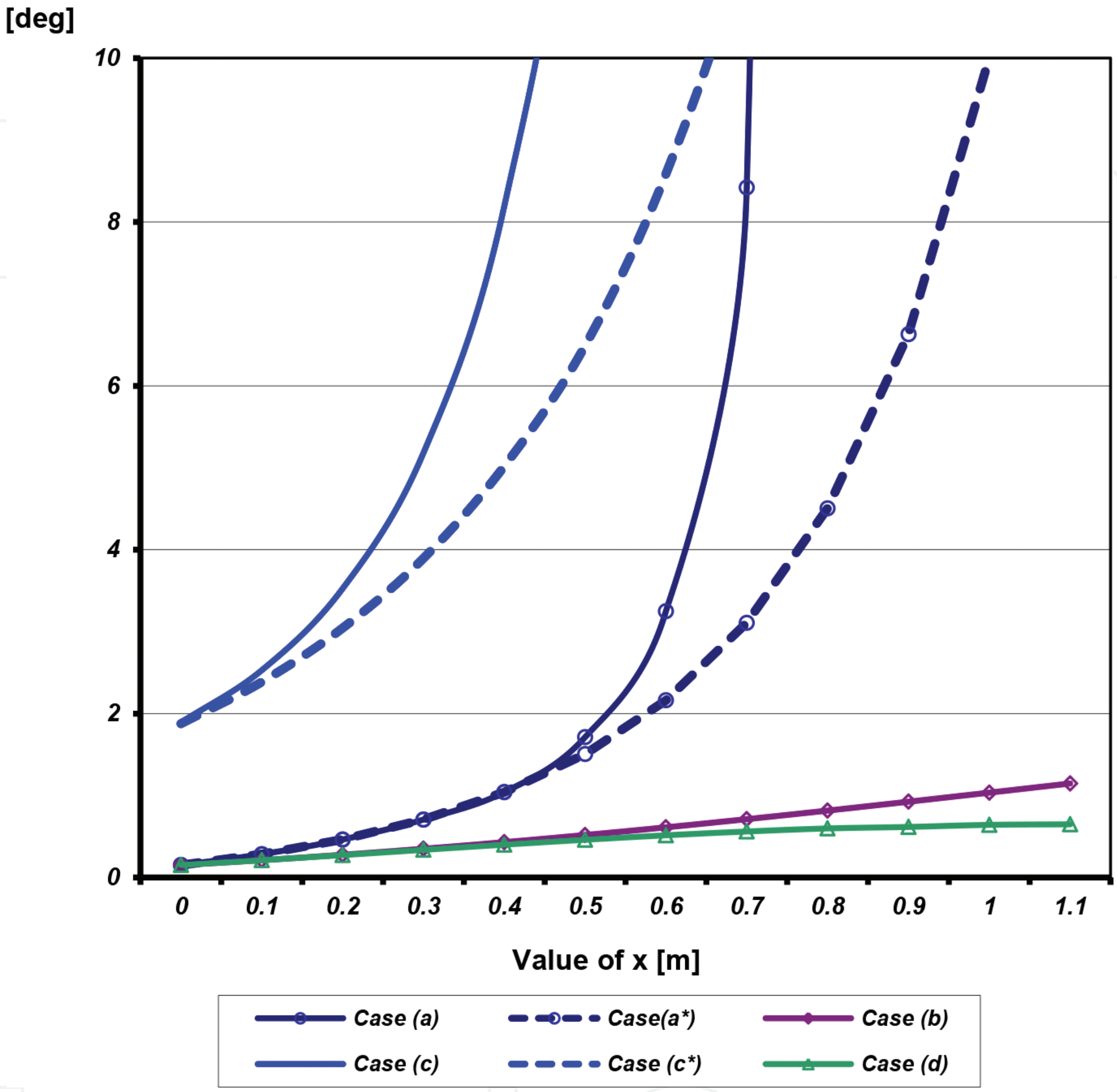

Figure 4. Dependency of the rotation of the foundation surface for *x* values.

2.3.2. Gradual decrease in the stiffness of the basement rock

In case (b) (see **Figure 2**), the interaction parameter C_z decreases gradually. The development of the C_z values is constant up to the place that is, in all likelihood, affected by water penetration. From that point onwards, the stiffness is linear up to the point 1 where the stiffness of the basement rock is assumed to be zero. Resulting values are listed in **Table 2**. The development of the values is shown in **Figure 4**.

2.3.3. Gradual washing-away of soil and washing-off of fine-grain particles

Combination of both the previous situations represents the case 'c'. Here, the C_z is considered to be constant below the point 1 (see **Figure 2**). The soil is washed off gradually, thus decreasing C_z. Resulting values are listed in **Table 3**. From the chart in **Figure 4**, it is evident that the tensile stress in the contact surface appears as early as in the first phase. The procedure has been similar to that used in case (a). An iteration method has been used for case (c). The case (c*) describes the situation where the basement rock is subjected to the tension.

x [m]	Origin (1.9 – x) [m]	w_1 [mm]	w_2 [mm]	$\Delta w = w_2 - w_1$ [mm]	Rotation of foundation [deg]	Max. stress on foundation surface [MPa]
0.0	1.9	6.92	11.98	5.06	0.152	0.299
0.1	1.8	6.29	13.30	7.02	0.212	0.321
0.2	1.7	5.60	14.81	9.21	0.278	0.344
0.3	1.6	4.88	16.52	11.64	0.351	0.364
0.4	1.5	4.12	18.42	14.31	0.431	0.381
0.5	1.4	3.33	20.54	17.21	0.519	0.396
0.6	1.3	2.53	22.85	20.32	0.613	0.405
0.7	1.2	1.74	25.36	23.63	0.712	0.410
0.8	1.1	0.96	28.05	27.09	0.817	0.409
0.9	1.0	0.22	30.90	30.69	0.925	0.401
1.0	0.9	–0.35	33.78	34.13	1.029	0.392

Table 2. Deformation of the foundation for the case ′b′.

x [m]	Origin (1.9 – x) [m]	w_1 [mm]	w_2 [mm]	$\Delta w = w_2 - w_1$ [mm]	Rotation of foundation [deg]	Max. stress on foundation surface [MPa]
0.0	1.9	–3.57	59.18	62.75	1.893	0.38
0.1	1.8	–9.10	74.74	83.84	2.530	0.427
0.2	1.7	–18.68	98.10	116.78	3.526	0.49
0.3	1.6	–36.13	135.23	171.35	5.181	0.574
0.4	1.5	–70.31	199.51	269.82	8.192	0.691
0.5	1.4	–141.30	319.79	461.09	14.184	0.861
0.6	1.3	–323.69	602.49	926.18	30.374	1.182
0.7	1.2	–669.93	1253.43	1923.36	91.693	2.009

Table 3. Deformation of the foundation for the case ′c′.

2.3.4. Step decrease in the parameters of the basement rock

Because the soil is saturated with water and fine-grain particles have been washed off, the stiffness will decrease (see **Figure 2**). In contrast to the calculation with the linear distribution (case ′b′), a step division of C_z has been chosen. When modelling by means of two parameters, the entering of values is simpler and faster. When modelling the linear development, the entering of values is more complex and C_z is different for each element. **Table 4** and **Figure 4** give the values for case ′d.

x [m]	Origin (1.9 – x) [m]	w_1 [mm]	w_2 [mm]	$\Delta w = w_2 - w_1$ [mm]	Rotation of foundation [deg]	Max. stress on foundation surface [MPa]
0.0	1.9	6.92	11.98	5.06	0.152	0.299
0.1	1.8	6.29	13.30	7.02	0.212	0.321
0.2	1.7	5.65	14.75	9.09	0.274	0.342
0.3	1.6	5.06	16.27	11.21	0.338	0.369
0.4	1.5	4.52	17.84	13.31	0.401	0.372
0.5	1.4	4.09	19.39	15.30	0.461	0.38
0.6	1.3	3.77	20.87	17.10	0.516	0.382
0.7	1.2	3.59	22.24	18.65	0.562	0.379
0.8	1.1	3.56	23.45	19.88	0.600	0.372
0.9	1.0	3.69	24.17	20.48	0.618	0.36
1.0	0.9	3.96	25.29	21.33	0.643	0.346

Table 4. Deformation of the foundation for the case 'd'.

3. Conclusion

Figure 4 summarises the results of the conditions described above. Also, the chart shows the rotation of the foundation surface. **Table 1–4** can be used to determine the values for a specific case and to determine the maximum stress that appears in the contact surface. The structure collapses if the basement rock plasticizes and the load-carrying capacity is lost. According to the limiting rotation requirements by CNI (1988), the ratio $\Delta w/b = 0.003$ applies to the concrete foundation structure. The rotation angle is $\phi = 0.17°$. It follows from the calculation that the structure does not meet this requirement when the x-parameter (case 'b') decreases below the foundation surface 0.1 m. This is the beginning of the condition when the fine-grained particles start washing away. Most adverse results occur in the case 'c' when the lower stiffness of the basement rock is combined with the loss of contact with the basement rock. Because of the lost contact between the foundation and basement rock, the stress re-distributes and tensile stress appear in the contact surface. It is clear from the chart that there is a difference in the calculations (case 'a' and case 'c') where the tensile stress is, or is not, considered for the contact surface. The situation where the tensile stress exists is marked with an asterisk. The results are absolutely different. Therefore, the tensile stress in the foundation surface should not be taken into account.

Conflict of interest

The authors declare that there is not conflict of interest.

Acknowledgement

The work was supported from sources for conceptual development of research, development and innovations 2016 at the VŠB-Technical University of Ostrava that were granted by the Ministry of Education, Youths and Sports of the Czech Republic. In this undertaking, theoretical results gained in the project GAČR 16-08937S were partially exploited.

Author details

Radim Cajka, David Pustka* and David Sekanina

*Address all correspondence to: david.pustka@vsb.cz

Faculty of Civil Engineering, VSB-Technical University of Ostrava, Ostrava, Poruba, Czech Republic

References

S. H. Afzali. New model for determining local scour depth around piers. Arabian Journal for Science and Engineering, 1–9, 2015, DOI: 10.1007/s13369-015-1983-4.

J. L. Briaud, P. Gardoni, and C. Yao. Statistical, risk, and reliability analyses of bridge scour. Journal of Geotechnical and Geoenvironmental Engineering, 140 (2), art. no. 0000989, 2015, DOI: 10.1061/(ASCE)GT.1943-5606.0000989.

S. E. Burns, S. K. Bhatia, C. M. C. Avila, B. E. Hunt, B.E., (eds.). Scour and Erosion–Proceedings of the Fifth International Conference on Scour and Erosion (ICSE-5). American Society of Civil Engineers (ASCE), 2011.

R. Cajka, P. Manasek. Building structures in danger of flooding. In: IABSE Symposium Report. International Association for Bridge and Structural Engineering, New Delhi, India. WOS: 000245746100072, 2005.

R. Cajka, V. Krivy, D. Sekanina. Design and development of a testing device for experimental measurements of foundation slabs on the subsoil. Transactions of the VŠB – Technical University of Ostrava, Civil Engineering Series, 11(1), 1–5, 2011, DOI: 10.2478/v10160-011-0002-2.

R. Cajka. Accuracy of stress analysis using numerical integration of elastic half-space. Applied Mechanics and Materials, 300–301, 1127–1135, 2013a, DOI: 10.4028/www.scientific.net/AMM.300-301.1127

R. Cajka. Analysis of stress in half-space using Jacobian of transformation and gauss numerical integration. Advanced Materials Research, 818, 178–186, 2013b, DOI:10.4028 /www.scientific.net/ AMR.818.178.

R. Cajka. Analytical derivation of friction parameters for FEM calculation of the state of stress in foundation structures on undermined territories. Acta Montanistica Slovaca, 18(4), 254–261, 2013c.

R. Cajka, K. Burkovic, V. Buchta and R. Fojtik. Experimental soil–concrete plate interaction test and numerical models. Key Engineering Materials, 577–578, 33–36, 2014.

R. Cajka, J. Labudkova and P. Mynarcik. Numerical solution of soil–foundation interaction and comparison of results with experimental measurements, International Journal of Geomate, 11(1), 2116–2122, 2016.

R. Cajka, P. Mynarcik, and J. Labudkova. Experimental measurement of soil-prestressed foundation interaction, International Journal of GEOMATE, 10(4), 2101–2108, 2016.

CNI. ČSN 73 1001 Foundation of structure. Subsoil under shallow foundations, Prague, 1988 (in Czech).

CNI. ČSN EN 1997-1 Geotechnical design–Part 1: General rules, Prague, 2004 (in Czech).

CNI. ČSN EN 1992-2 Design of concrete structures–Concrete bridges–Design and detailing rules, Prague, 2005 (in Czech).

J. Collins, M. Steele, D. Wilkes, D. Ashurst and B. Harvey. Investigation into highway bridge damage and failures during the November 2009 Cumbria flood event. In: Forensic Engineering–Informing the Future with Lessons from the Past–Proceedings of the Fifth International Conference on Forensic Engineering organised by the Institution of Civil Engineers and held in London, UK. ICE Publishing, pp. 49–60, 2013.

M. Ehteram, A. M. Meymand. Numerical modeling of scour depth at side piers of the bridge, Journal of Computational and Applied Mathematics, 280, 68–79, 2015, http://dx.doi.org/10.1016/j.cam.2014.11.039.

R. Ettema, R. Arndt, P. Roberts and T. Wahl (eds.). Hydraulic Modeling–Concepts and Practice. American Society of Civil Engineers (ASCE), ISBN 0-7844-0415-1, 2000.

C. Fael, R. Lança and A. Cardoso. Effect of pier shape and pier alignment on the equilibrium scour depth at single piers, International Journal of Sediment Research, 1–7, 2016, http://dx.doi.org/10.1016/j.ijsrc.2016.04.001.

FEM consulting, 2002. Nexis 32 rel.3.50 - Soilin. Manual for software, SCIA group.

E. Hrubesova, H. Lahuta, L. Duris and M. Jaafar. Mathematical modeling of foundation-subsoil interaction. In: International Multidisciplinary Scientific GeoConference Surveying Geology and Mining Ecology Management, SGEM, 2 (1), pp. 437–444, 2015.

E. Hrubesova, J. Marsalek and J. Holis. The influence of inaccuracies of soil characteristics on the internal forces in the retaining wall. In: Advances and Trends in Engineering Sciences and Technologies–Proceedings of the International Conference on Engineering Sciences and Technologies, ESaT 2015, pp. 69–74, 2016.

P. Janas, M. Krejsa, V. Krejsa and R. Briš. Structural reliability assessment using direct optimized probabilistic calculation with respect to the statistical dependence of input variables. In: Safety and Reliability of Complex Engineered Systems–Proceedings of the 25th European Safety and Reliability Conference, ESREL 2015, pp. 4125–4132, 2015.

A. Khosronejad, S. Kang, and F. Sotiropoulos. Experimental and computational investigation of local scour around bridge piers, Advances in Water Resources, 37, 73–85, 2012, http://dx.doi.org/10.1016/j.advwatres.2011.09.013.

J. V. Klinga, A. Alipour. Assessment of structural integrity of bridges under extreme scour conditions. Engineering Structures, Volume 82, 55-71, http://dx.doi.org/10.1016/j.engstruct.2014.07.021, 2015.

P. Koteš, J. Vičan, and M. Ivašková, M. Influence of reinforcement corrosion on reliability and remaining lifetime of RC bridges. Materials Science Forum, 844, 89–96, 2016, DOI: 10.4028/www.scientific.net/MSF.844.89.

J. Králik and J. Králik Jr. Failure probability of NPP communication bridge under the extreme loads. Applied Mechanics and Materials, 617, 81–85, 2014, DOI: 10.4028/www.scientific.net/AMM.617.81.

J. Labudkova and R. Cajka. Experimental measurements of subsoil-structure interaction and 3D numerical models, Perspectives in Science, 7, 240–246, 2016, http://dx.doi.org/10.1016/j.pisc.2015.11.039.

H. Lahuta, E. Hrubesova, L. Duris, L. and T. Petrasova. Behaviour subsoil of slab foundation under loading, In: International Multidisciplinary Scientific GeoConference Surveying Geology and Mining Ecology Management, SGEM, 2 (1), pp. 119–126, 2015.

Ch. Lin, J. Han, C. Bennettand R. L. Parsons. Case History Analysis of Bridge Failures due to Scour. In: Proceedings of the International Symposium of Climatic Effects on Pavement and Geotechnical Infrastructure 2013. American Society of Civil Engineers (ASCE), pp. 204–2016, 2014.

O. Link, F. Pfleger and U. Zanke, U. Characteristics of developing scour-holes at a sand-embedded cylinder, International Journal of Sediment Research, 23(3), 258–266, 2008, http://dx.doi.org/10.1016/S1001-6279(08)60023-2.

J. Markova, M. Holicky, M. Sykora, and J. Kral. Probabilistic assessment of traffic loads on bridges. In: Safety, Reliability and Risk Analysis: Beyond the Horizon–Proceedings of the European Safety and Reliability Conference, ESREL 2013, pp. 2613–2618, 2014.

Y. A. Mohamed, G. M. Abdel-Aal, T. H. Nasr-Allah and A. A. Shawky. Experimental and theoretical investigations of scour at bridge abutment, Journal of King Saud University–Engineering Sciences, 28(1), 32–40, 2016, http://dx.doi.org/10.1016/j.jksues.2013.09.005.

J. Navratil. Structural analysis of bridges, legitimate conservatism and obsolete theories. Concrete Engineering International, 8(1), 17–19, 2004.

J. Navratil and M. Zich. Long-term deflections of cantilever segmental bridges. Baltic Journal of Road and Bridge Engineering, 8(3), 190–195, 2013, DOI: 10.3846/bjrbe.2013.24.

G. Parke, H. Nigel. ICE Manual of Bridge Engineering (2nd Edition). ICE Publishing, Thomas Telford Ltd, 1 Heron Quay, London E14 4JD, UK 2008.

R. Pasiok, and E. Stilger-Szydlo. Sediment particles and turbulent flow simulation around bridge piers, Archives of Civil and Mechanical Engineering, 10(2), 67–79, 2010, http://dx.doi.org/10.1016/S1644-9665(12)60051-X.

D. Pustka, R. Cajka, P. Marek and L. Kalocova. Multi-components load effect analysis on a slender reinforced concrete column using probabilistic SBRA method. In: EASEC-11–Eleventh East Asia-Pacific Conference on Structural Engineering and Construction. Taiwan, 19, pp. 334–335, 2008.

D. Pustka. Probabilistic reliability analysis of high-performance reinforced concrete beam using Matlab software. International Journal of Mechanics, 8, 101–111, 2014.

D. Pustka. Probabilistic approach to stability analysis of a reinforced concrete retaining wall. Advanced Materials Research, .1079–1080, 248–251, Trans Tech Publications, Switzerland, 2015, doi:10.4028/www.scientific.net/AMR.1079-1080.248.

V. Raizer. Reliability of Structures. Analysis and Applications. Backbone Publishing Company, Fair Lawn, USA, ISBN 978-09742019-7-9, 2009.

J. Strasky, J. Navratil and S. Susky. Applications of time-dependent analysis in the design of hybrid bridge structures. PCI Journal, 46 (4), 56–74, 2001.

O. Sucharda and J. Brozovsky. Bearing capacity analysis of reinforced concrete beams. International Journal of Mechanics, 7(3), 192–200, 2013.

P.J. Tikalsky, D. Pustkaand Pavel Marek. Statistical variations in chloride diffusion in concrete bridges. ACI Structural Journal, 102(3), 481–486, 2005.

T. Unlu, H. Akcin, and O. Yilmaz. An integrated approach for the prediction of subsidence for coal mining basins. Engineering Geology, 166, 186–203, 2013, DOI: 10.1016/j.enggeo.2013.07.014.

C.Y. Wang, J.H. Cheng, H.P. Shihand J.W. Chang. Ring columns as pier scour countermeasures, International Journal of Sediment Research, 26(3), 353–363, 2011, http://dx.doi.org/10.1016/S1001-6279(11)60099-1.

X. Yu, J. Tao and X. Yu. Comparison Study on Computer Simulations for Bridge Scour Estimation. In: Proceeding of Georisk 2011–Geotechnical Risk Assessment & Management. American Society of Civil Engineers (ASCE), pp. 1125–1132, 2011.